Chapter

The Mid-Infrared Photonic Crystals for Gas Sensing Applications

Tahere Hemati and Binbin Weng

Abstract

Mid-infrared spectrum is known as the "molecular fingerprint" region, where most of the trace gases have their identical absorption patterns. Photonic crystals allow the control of light-matter interactions within micro/nanoscales, offering unique advantages for gas analyzing applications. Therefore, investigating mid-infrared photonic crystal based gas sensing methods is of significant importance for the gas sensing systems with high sensitivity and portable footprint features. In recent various photonic crystal gas sensing techniques have been developing rapidly in the mid-infrared region. They operate either by detecting the optical spectrum behavior or by measuring the material properties, such as the gas absorption patterns, the refractive index, as well as the electrical conductivities. Here, we will brief the progress, and review the above-listed photonic crystal approaches in the mid-infrared range. Their uniqueness and weakness will both be presented. Although the technical level for them has not been ready for commercialization yet, their small size, weight, power consumption and cost (SWaP-C) features offer great values and indicate their enormous application potentials in future, especially under the stimulation of the newly emerging technology "Internet of Things" which heavily relies on modern SWaP-C sensor devices.

Keywords: mid-infrared, photonic crystal, gas sensing, non-linear light, nanophotonics

1. Introduction

Chemical sensing, especially the trace-gas detection, is of a significant importance for a wide range of applications in practical fields including the medical inspection, the environmental monitoring, the manufacturing control, as well as the nation security surveillance. For example, controlling respiratory gases in the medical sector can be a matter of life or death [1, 2]. Monitoring the toxic, explosive and air polluting gases such as NO_x, CO_2, CO, CH_4, and O_3 is vital to prevent harms to human communities [2]. Nowadays, there are many choices of gas sensors based on different methods such as semiconductor [3, 4], catalytic [5], field effect [6], electrochemical [7], and optical gas sensors [8, 9]. Among them, the optical-based gas sensors have been well-received as a fast, precise and reliable technique, which has a long life expectancy, immunes to all chemical poisoning,

and requires low maintenance for high-precision operation [9]. Furthermore, with the rise of the emerging technology, Internet of Things (IoTs), such high standard of performance requirements become more and more desired from the industrial world [10]. It is also necessary to point out that, besides of the aforementioned features, the importance of reducing the size, weight, power, and cost (SWaP-C) to enable the chip scale integration is revealed clearly in the development of IoT technologies [11]. Unfortunately, limited by the Beer-Lambert Law, to achieve a suitable sensitivity, a large optical interaction length is required in the conventional optical gas sensor systems. This long path of interaction makes the optical gas sensors relatively large and costly to be manufactured [12], which consequently sets a fundamental barrier to satisfy the SWaP-C requirements. Therefore, in such a high-speed technology innovating era, more and more researchers have paid significant attention to develop new technologies that can overcome these limitations.

Photonic crystals (PhCs), which can be regarded as one of the most advanced modern photonic technologies [13–16] was firstly proposed by Yablonvitch and John since 1980s [17, 18]. Owing to the unique non-linear optical dispersive properties [19, 20], PhCs become a powerful tool for control and manipulation of light-matter interactions on micrometer length scales [21, 22]. Considering the aforementioned optical sensing limitations, this technology is capable of addressing the size issue, and potentially suitable for on-chip gas detection applications. In recent year, the research on PhC-based gas sensing research has developed rapidly. Various sensing techniques have been proposed by using PhCs to detect chemicals in gas, vapor and even liquid environment [23–25]. Several review articles have been reported as well [26, 27]. For example, in 2013, Xu et al. [27] investigated different photonic crystal structures, such as morpho-butterfly wing, porous silicon PhCs, multilayer PhC films, colloidal PhCs, and Inverse opal colloidal crystals. In 2015, Zhang et al. [26] reviewed optical sensors based on photonic crystal cavity enhancing mechanisms. Overall speaking, the reported technologies can be considered in two categories. The first approach can be concluded as the "refractive index sensing", which could sensitively measure refractive index changes with gas involvement. Another one is known as "photonic crystal light absorption spectroscopy". This method is to detect the distinctive absorption patterns of gas molecules in the infrared spectrum. Because photonic crystals can slow light propagation and enhance light intensity in the space where gas fills [4], this new spectroscopy not only shares the advantages of the conventional spectroscopy but also eliminates the issues caused by large optical interaction length.

To the best of our knowledge, the research emphasis on the PhC-based gas sensing development has been mainly focused on the near-infrared spectral range. However, compared with the near-infrared region, molecular species in the mid-infrared range show intrinsic absorption bands with much larger absorption coefficients. **Figure 1** presents that the mid-infrared portion of the spectrum with several trace gas chemical species placed where their strong absorptions occur. As can be seen, taking the carbon dioxide (CO_2) as an example, its absorption strength in the mid-infrared range (~4.2 μm) is about two orders of magnetite higher than the one in near-infrared range (~2 μm). Such significant difference also exists in almost all the gas molecules including xylene, methane, and so on [29]. Therefore, fundamentally speaking, the optical sensors functioning in the mid-infrared range offer much higher device sensitivity [30]. Consequently, much richer information can be found for those wishing to probe, detect, image, or quantify these and many other species including explosives, nerve agents, and toxins [30]. Nevertheless, there are some hurdles preventing the development of PhC based optical sensors in

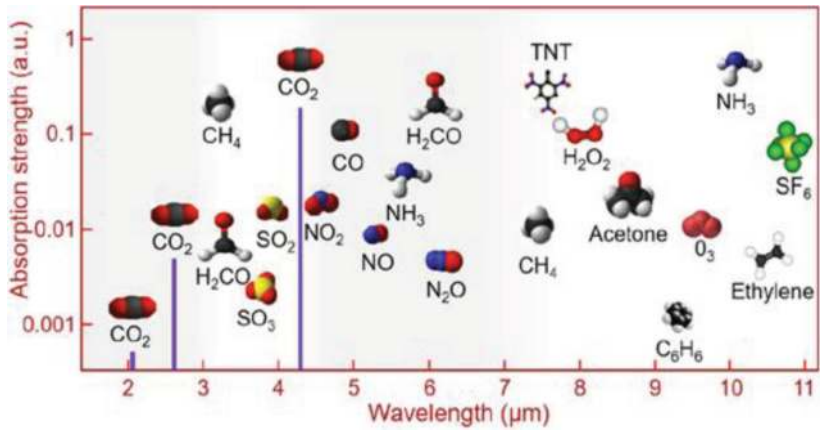

Figure 1.
The absorption strength of some typical trace gas molecules in the mid-infrared range [28].

the mid-infrared spectrum, such as the limited availability of the low-cost, high-efficient light sources or photodetectors. Also, it was pointed out in a report that the difficult process of alignment of the beam for coupling light in and out of the sample could also be very challenging, due to limitations of available equipment [31]. In order to have a systematic understanding of the current progress of PhC based gas sensing research in mid-infrared range, in this chapter, we are going to provide a comprehensive review on the existing mid-infrared PhC-based gas sensor technologies, evaluate their performance in a practical point of views, and also discuss the future of the PhC-based mid-infrared sensing technologies.

2. PhC-based mid-infrared gas sensing methods

It is known that most of the molecules have their distinctive absorption patterns in the mid-infrared spectrum, and as it was pointed out that their absorption coefficients are much higher than the ones in near-infrared range. Majorly due to these reasons, the most active research efforts of using PhC technology for gas sensing in mid-infrared range focuses on measuring the spectral intensity change caused by the gas resonant mode absorption mechanisms. But it is necessary to point out that, other than this typical methodology, some other approaches using PhC structures have also been reported, which rely on the detection of the peak position drifting of transmission or reflection spectrums caused by the gas-induced refractive index variation, or the electrical conductance behavior in the presence of gases. These methods certainly help to enrich the PhC sensing capabilities in the mid-infrared range. With all these being said, based on the different sensing mechanisms, in the following contents, we will elaborate on the recent development of the mid-infrared PhC based gas sensing technologies.

2.1 Mid-infrared light absorption sensing

Being as the most popular technology in the mid-infrared range, the gas absorption spectroscopy can be used to precisely measure both the gas composition and concentrations. In this method, the mid-infrared radiation is absorbed at some specific frequencies due to the presence of gas molecules. These frequencies correspond to vibrational modes of the molecular structures [32]. Typically, this type of gas sensor consists of three parts: the mid-infrared light source, the light/gas interaction

chamber, and the radiation detector [33]. In recent years, PhC has been proven to be an effective technology to improve the performance of the light sources, especially for the laser devices [34]. But more significantly, PhC has also played a critical role to downsize the sensor module footprint by minimizing the interaction chamber volume under the chip scale level [35–38].

2.1.1 Advanced porous gas sampling structure for gas sensing

As proposed by Soref [29], silicon is a proper candidate for the mid-IR wavelength range due to its transparency window between 1.1 and 8.5 μm. While silicon dioxide is also transparent up to around 3.6 [29], silicon-on-insulator (SOI) is a suitable structural form for mid-IR integrated photonics [39]. In 2007, Lambrecht et al. [12] for the first time, suggested the implementation of a two dimensional (2D) macroporous silicon PhC in the interaction volume to slow the light and enhance the gas-light interaction. The experimental results with CO_2 showed more than two times enhancement in absorption line. In fact, these experimental results became a base for the realization of high sensitivity and miniature gas sensors. The device configuration is shown in **Figure 2**. Gas flows through the sampling cell from the top hole to the bottom, as highlighted in blue color. The sampling cell containing a PhC membrane is positioned between a thermal emitter and a pyrodetector with an IR bandpass filter centered at the absorption peak of CO_2 (λ = 4.24 μm). The PhC membrane is placed in between two BaF_2 light guiding rods which help to couple the IR radiation among the thermal emitter, PhC membrane and the pyrodetector. Here, one thing is worth noting that, the PhC membrane could be easily removed from the plastic holder without changing positions of the BaF_2 rods. This offers the possibility of measuring the empty cell with the same optical path length. In detail, the operation voltage is 10 Hz and the pyrodetector is measured by digital lock-in amplifier with a time constant of 2 s. With such setup, this method does offer the capability to detect the presence of CO_2 gas, which proves the possibility of using PhC technology for developing gas sensors with compact footprint. However, there is a crucial drawback with this simple PhC gas sensor. Typically, a low group velocity corresponds to a high effective refractive index, which leads to difficulties in and out couplings of radiation.

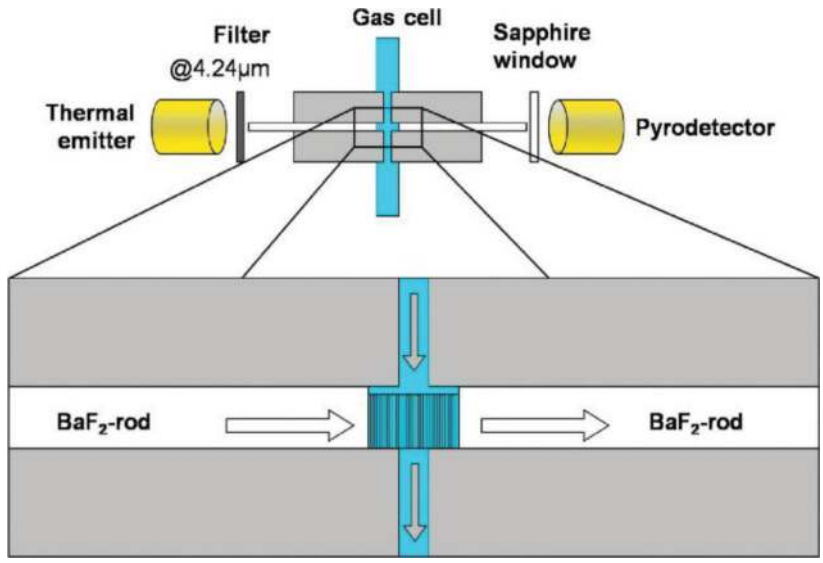

Figure 2.
Schematic design used for gas absorption measurements [35].

In 2011, Pergande et al. [35] solved this problem via designing antireflection layers (ARL) at two interfaces, including the air-ARL interface and the ARL-PhC interface. Because of that, it enhanced the light absorption of CO_2 up to 3.6 times. To explain the mechanism, introducing this ARL leads to the generation of surface modes which are used for coupling light into slow light PhC modes. These modes are confined in air-ARL interference due to the forbidden propagation of light in photonic band-gap. The thickness of ARL affects the spectral position of surface modes. When ARL thickness is equal to 0.57a (a is the lattice constant of PhC), the similarity of field distributions of surface modes and the slow light PhC modes would be able to couple together much easily. In addition, this ARL could also help to effectively reduce the interface optical loss. Theoretically, absorption of the device can be enhanced up to 60 by using this ARL enhanced PhC configuration. The difference between theoretical and experimental results comes from several factors, such as the non-optimal lattice constant and pore diameter fluctuation. They all could lead to the off-resonance operation mode to the CO_2 absorption line. In this work, 2D PhCs were fabricated by photoelectrochemical etching of n-type silicon. ARL is designed by photolithography and was transferred by photoelectrochemical etching into the silicon wafer. The lattice constant was 2 μm an (r/a), varying from 0.360 to 0.385. lengths of PhC changed from 100 μm to 1 mm while the height and width were approximately 330 μm and 1 mm, respectively. The porosity of the sample was about 64%. Pergande et al., according to numerical estimates, suggested that the positional variations and pore diameter fluctuations should be below 0.5% in order to allow for a reasonable transmission in the 1 mm device.

In the course of the experiment, several sample lengths, varying from 0.25 to 1 mm, were investigated. Results showed that their absorption enhancements changed at the range of 2.6–3.5. By taking all the mismatch factors into consideration, the numbers are in good agreement with the numerical simulation results. All the data are presented in the following **Table 1**.

In 2000, Boarino et al. [40] applied this porous silicon method to the environmental analysis of NO_2 gas because of its high sensitivity to surface molecular structures. **Figure 3** shows the enhanced absorption value due to the presence of NO_2. In this figure, spectrum-1 is related to the sample outgassed under dynamic vacuum, spectrum-2 is given after the dosage of 1 Torr of the pure NO_2 sample, and spectrum-3 is recorded after outgassing. As can be seen, in the range of 1000–1250 cm^{-1} (assigned to the stretching vibrations of Si–O species) and range of 2150–2300 cm^{-1} (Si–H stretching modes of SiO–H_x species) the absorption enhancement in the presence of NO_2 is intense while this value, at 3748 cm^{-1} (SiO–H stretching vibration), is negligible. They claimed that this broad absorption can be attributed to electrons populating of the conduction band. Moreover, from spectrum-3 is an evidence that removing NO_2 from the gas phase leads to a complete restoration of initial conditions. Moreover, the most recent research based on this method showed the enhanced gas absorption by a factor of 5.8 at 5400 nm [41].

It can be concluded that porous silicon is an effective gas sampling structure that can help in minimizing the overall size of the sensor device. However, the main

Length (mm)	Gas	Filter[μm/(a/λ)]	ζ_{exp}	$\zeta_{theo,TM}$	$\zeta_{theo,TE}$
1	CO_2	4.24/0.472	3.5	3.7	2.9
0.5	CO_2	4.24/0.472	2.6	3.7	2.9
0.5	CO_2	4.24/0.472	3.0	3.7	2.9

Table 1.
Experimental and theoretical value of the gas absorption enhancement [35].

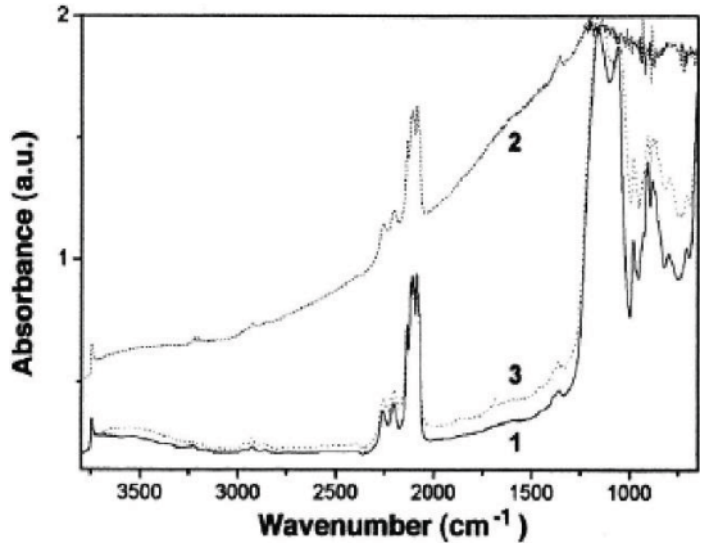

Figure 3.
FTIR spectra of free-standing p + PSL: Spectrum-1 is related to sample outgassed under dynamic vacuum. Spectrum-2 has been obtained after dosage of 1 Torr of pure NO_2, spectrum-3 has been recorded after outgassing the sample, under dynamic vacuum [40].

restrictive factor for using porous silicon PhCs in gas sensing is its high sensitivity to the small fluctuation of the pore diameter and the lattice constant. For instance, more than 0.5% pore diameter fluctuation in the 1 mm device eliminates the advantage of using the porous silicon. Thus, a high technology is needed for fabricating this porous silicon, which limits the implementation of this method. However, for cases where high-sensitive and small sensors are needed, using porous silicon PhCs to decrease the interaction path and increase the sensitivity is a suitable option.

2.1.2 Photonic crystal waveguide (PCW) for gas sensing enhancement

Mid-IR PhC waveguides (PCW) with high-quality factor are powerful tools for nonlinear optical applications because they can achieve slow-light enhancement and low linear propagation loss simultaneously [31]. Therefore, this component is of major interests in the gas sensing research area. The enhanced detection sensitivity achieved by using PCWs (strip and slot waveguides) in the near-infrared range have been previously reported [42, 43]. However, based on our knowledge, very few works about the PCW enhanced gas sensor in the mid-infrared range has been reported so far [44]. In 2015, Zou et al. [45] provided the first experimental demonstration of transmission characteristics of holey and slotted PCWs in silicon-on-sapphire at the wavelength of 3.43 μm with a fixed-wavelength inter-band cascade laser (ICL). They used an 800 μm long holey PCW to detect gas-phase Triethyl phosphate (TEP) with the concentration of 10 ppm (parts per million).

They investigated a holey PCW with a row of smaller holes (r_s = 0.65r), which was located in the center of PCW (hexagonal lattice of air holes in silicon) where air hole radius was r = 0.25*a* (*a* is lattice constant). As shown in **Figure 4** the optimization of (r_s/r) value has been conducted through considering four conditions: having a large guiding bandwidth for the propagating PCW modes, broad mode bandwidth, large electrical field overlap with the analyte, and high peak enhancement factor which yield to more efficient light-matter interaction. The other value that should be optimized is the lattice constant. As shown in **Figure 5** for a less than 830 nm, due to stopgap, there is no transmission. Moreover, when *a* is located between 840 and 845 nm the propagation loss is approximately 15 dB/cm, while

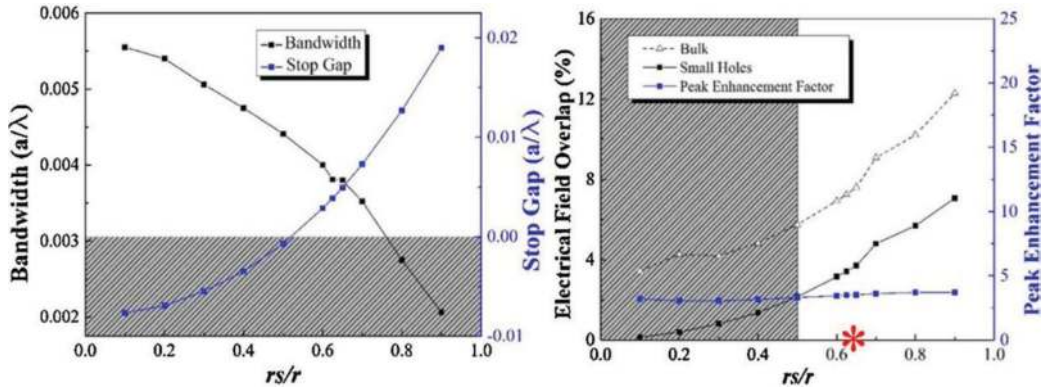

Figure 4.
Optimization of r_s/r according to bandwidth, stop gap electrical field overlap, peak enhancement factor [45].

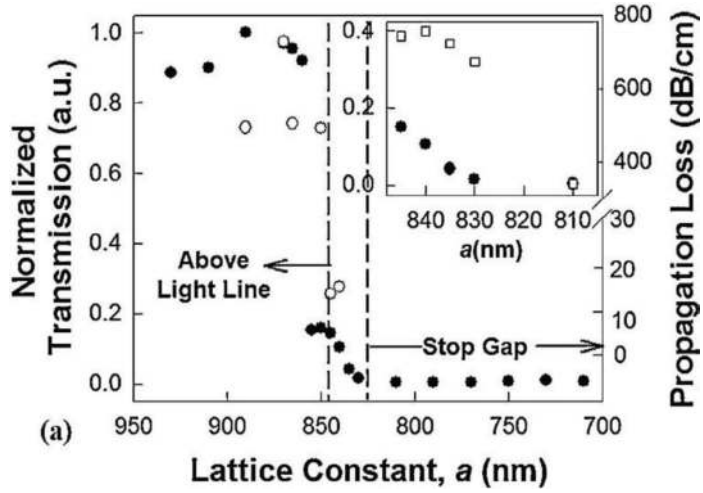

Figure 5.
Lattice constant dependent transmission and propagating loss [45].

this value increases dramatically for a > 845 nm. Therefore, it can be concluded that in order to have reasonable transmission and propagation loss, the lattice constant should have a value between dashed lines in **Figure 5**.

On the other hand, the slotted type PCW was also investigated. Likewise, the same optimization process was conducted for slotted PCW to determine slot width (130 nm) and lattice constant (between 830 and 840 nm). However, the optimized value showed propagation loss of 55 dB/cm, which is almost 3 times greater than the loss propagation in holey PCW. Afterward, they compared the peak of electric field enhancement factor in the holey PCW, and the conventional rectangular slotted PCW, to a regular PCW. This comparison showed 3.5 times and 13 times enhancement for holey and slotted PCW (respectively) relative to regular PCW. Furthermore, the electrical field overlap with the analyte in regular PCW was 5%, while this value for holey and slotted one was 8 and 15% respectively. However, propagation loss for holey PCW was 15 dB/cm while this value was 55 dB/cm for slotted one. Thus, we can conclude that the holey PCW can be a better candidate for absorption spectroscopic gas sensing because while its electrical field overlap with the analyte is 2 times lower than slotted PCW, the propagation loss of slotted PCW is 3 times higher than holey PCW.

The transmitted light through an 800 μm long holey PCW with a = 845 nm is measured in the presence and absence of TEP. They investigated changes in

transmitted light intensity at λ = 3.43 μm for switching and steady state TEP flow through the holey PCW. For the switching flow, transmitted signal intensity dropped to 80% of its original intensity due to the presence of TEP. However, for the steady-state condition, this value dropped to 60% of its original value. Also, the measurements are independent of the flow rate of nitrogen at 10 and 50 ppm respectively. The noise in measurement comes from the electrical noise of detector and the vibration of the optical fiber. Furthermore, by replacing the slot and strip waveguide for the steady-state gas flow, instead of the holey PCW, just a small change in intensity of transmitted light at 3.43 μm is observed at 28 ppm TEP concentration. Thus, as **Figure 6** shows, it can be concluded that the holey PCW shows more sensitivity relative to the slot and strip waveguide because the holey PCW enhances both f (fill factor denoting relative fraction of optical field residing in the analyte medium) and group index, which is inversely related to group velocity. However, the slot waveguide only enhances the f factor, and has no impact on group index. Moreover, the high detection capability of PCWs in gas sensing is revealed in [46] where the detection of carbon monoxide with the concentration of parts-per-billion is possible.

In comparison to the porous silicon PhC Sensing method which enhances the sensor performance by only reducing group velocity, the PCW, especially the holey PCW, shows higher sensitivity because it enhances both f (filling factor denoting relative fraction of optical field residing in the analyte medium) and group velocity reduction simultaneously. In fact, using a PCW, instead of a simple 2D PhC, enables us to confine light and gas in at the same place, and increase the possibility of the interaction. Moreover, the propagation loss in PCWs is lower than the porous silicon PhC. However, the fabrication and optimization of a PCW are more complicated than the porous silicon PhC which potentially can lead to higher costs for PCW gas sensor development.

2.1.3 Mid-infrared PhC fiber enhanced sensing

Optical fibers offer significant advantages for gas sensing majorly due to its ability to confine optical radiation across long distances. It eliminates the need for beam collimation thus reduces device complexity significantly. However, their performance can be limited due to low mechanical flexibility, a weak overlap between light and gas or the requirement for conventional extrinsic gas cells [47]. Also, most of the fibers operate below 2 μm demonstrated due to the limited silica transmission window. In contrary to other microstructured fiber, Photonic bandgap fibers (PBFs) guide light in a gas (air) core rather than solid [48, 49]. This leads to the integration of gas sampling cell into the fiber, and the confinement of over 99% of the light in the hollow area rather than the silica, which makes PBFs an ideal

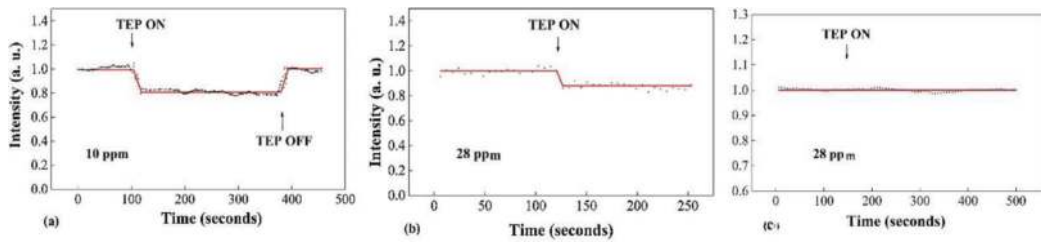

Figure 6.
(a). Change in transmitted light intensity through an 800 μm long holey PCW with a = 845 nm with 10 ppm TEP (b). Transmitted light intensity through a silicon slot waveguide in SoS in the presence and absence of 28 ppm TEP. (c). Transmitted light intensity through a silicon strip waveguide in SoS in the presence and absence of 28 ppm TEP [45].

candidate for miniaturized gas sensing applications [50, 51]. Furthermore, compared with the fused silica, these fibers can transmit light in the mid-infrared with a much lower optical loss (<1 dBm^{-1}) [52, 53].

Shephard et al. reported a bandgap guidance at 3.14 μm in a silica-based air-core photonic crystal fiber in 2005 [54]. The year after, they then investigate the gas sensing functionality using this PBF technology [53, 55]. The optical guiding range of this PBF was specially developed for methane sensing at ~3.2 μm [55]. The hollow-core PBF sensing unit was able to measure the methane vapor with the concentration of 1000 ppm. In the experiment, several fibers with a core diameter of ~45 μm and a pitch (distance between two neighboring cladding holes) between 7 and 8 μm were examined thoroughly. First, an 80 cm PBF was filled with the mixture of methane and nitrogen with the ratio of 5 (methane) to 95 (nitrogen) at the pressure of 2 bar. Then, the fiber was filled with nitrogen to normalize the measurements. The results are shown in **Figure 7** for 5, 1, 0.5, and 0.1% methane concentration. (solid curve) shows experimental results and the calculated absorption demonstrated by the dashed curve. Even in this low concentration (**Figure 7d**), the main absorption line of methane close to 3.32 μm is still visible, and the transmission dropped to significantly at this wavelength. Moreover, authors claimed that the small difference between the theoretical and experimental results is due to although processing errors during the spectral concatenation procedure.

In comparison to the porous silicon PhC as well as the PCW sensing mechanisms, the PBF gas sensor shows a higher energy overlap with gases and a lower optical loss. However, fibers are long in nature and this can be an obstacle to realization of SWaP sensors. Moreover, the degree of complexity for fabrication of PBFs can be lower than PCWs but is still higher compared to the porous silicon PhC devices.

2.2 Mid-infrared "refractive index" sensing

Besides of exploring the use of PhCs in the mid-infrared spectroscopy, there is another popular approach measuring the shift of PhC modulated Bragg resonant peak due to the refractive index change, which can lead to the detection of gas

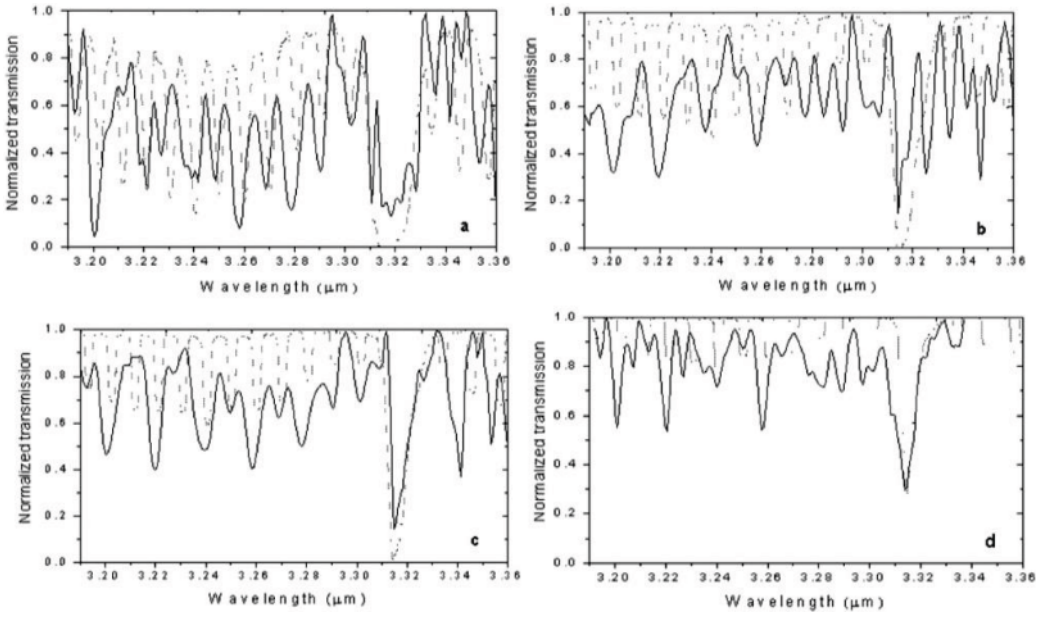

Figure 7.
Measured (solid curves) and theoretical (dash curves) absorption lines of methane for concentrations of a, 5%; b, 1%; c, 0.5%; and d, 0.1% [55].

concentrations. For instance, in a porous silicon PhC, when pore areas are filled by a gas the effective refractive index of the PhC will be increased. Moreover, it is possible that the lattice constant of the PhC increase due to the swelling of the gas or vapor. Understanding this procedure can be easier by considering Bragg law expression [27].

$$m\lambda = 2nd\sin\theta \quad (1)$$

where m is the diffraction order, λ is the incident wavelength, n is the effective refractive index, d is the lattice constant, and θ is the glancing angle between the incident light and diffraction crystal planes [56, 57]. This method has been used in near and visible range [58–60], more frequently rather than mid-infrared range.

In 2015 Zou et al. [45] designed a holey, slotted, and a regular PCW for detection the chemical warfare simulant in the mid-infrared range. A section of this research has been assigned to the investigation of the relationship between the value of electrical field overlap with the analyte and the sensitivity of the refractive change based sensors. In order to study this correlation, they used 3D FDTD simulation. They selected C_2Cl_4 (refractive index = 1.5) as a top cladding. As shown in **Figure 8** the sensitivity of a PCW sensor is depended directly on the percent of electrical field overlap with the analyte. So that, the shifted transmission in slotted PCW is 2 times higher than holey one because its electrical field overlap with the analyte is almost 2 times higher as well. In 2017 Turduev et al. [61] presented an optical refractive index sensor (T-slotted PC sensor) design for mid-IR photonics. They used numerical methods based on finite-difference time-domain and plane-wave expansion method. an overall sensitivity is calculated to be around 500 nm/RIU for the case of higher refractive indices of analytes n = 1.10–1.30.

Detecting an unknown gas through this method can be challenging because the principles of this method are based on the refractive index changes. Thus, detecting two different gases with the same refractive index is simply impossible. On the other hand, for gases with refractive indexes close to air refractive indexes (n = 1), the sensitivity of this kind of sensors can be strongly reduced. However, the complexity of this method is lower than absorption-based sensing methods.

2.3 Mid-infrared electrical conductance sensing

In 2000 Boarino et al. [38] studied changes in electrical conductivity in the presence of NO_2 through P^+ porous silicon layers (PSL) at the room temperature and the atmospheric pressure. The recovery time and response to interfering gases were tested as well. PSL is well-known in humidity sensors area, while its application in the field of gas sensing has been considered only recently. This structure has obtained high importance in the field of gas sensors due to its high surface to

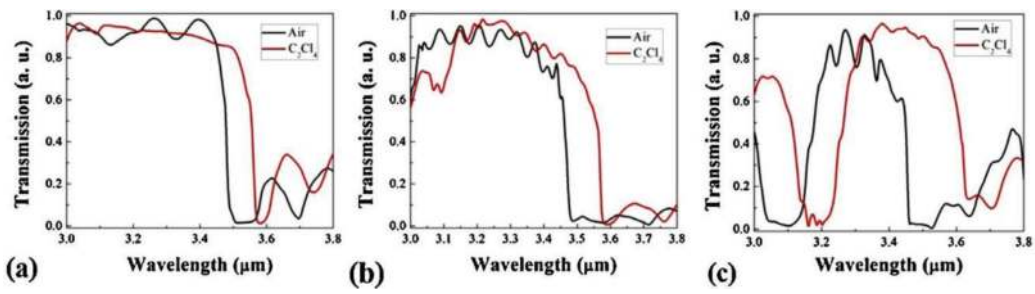

Figure 8.
Simulated transmission with air-clad and C_2C_{l4}-clad conditions for (a) conventional PCW, (b) holey PCW, and (c) slotted PCW [45].

Porosity (%)	ΔG/G (3 ppm)	ΔG/G (5 ppm)	ΔG/G (10 ppm)
38	6	87,837	0.7
43	1	1.9	3.5
53	0.3	1.7	4.6
62	29.3	84.3	197
75	3.5	45	164

Table 2.
Relative response of PS samples of different porosity to the listed NO_2 concentrations [38].

volume ratio, and its reactivity to the environment. Changes in work function, refractive index, photoluminescence, and conductivity variation can be used as indices in the gas sensing. Boarino et al. used the last feature to detect NO_2. Accordingly, due to the inherent characteristic of P^+ mesoporous silicon, strong changes can be observed in resistivity in the presence of polar liquids, vapors, and gases. They measured the PS change of conductance in presence of different gases in humid conditions at constant bias V = 5 v. The PS response to NO_2 was tested for different value of porosity. **Table 2** shows the relative conductance variation (ΔG/G) for different porosity (38, 43, 53, 62 and 75%).

Since the high available surface for gas adsorption plays a key role in obtaining an efficient chemical sensor, the 55% porosity for PS surface gives the best result, due to the maximum value of surface to volume ratio. The lowest concentration that could be examined, was 1 ppm and the relative response was 1.6 for the 60% porosity sample. In comparison with NO_2, under the same concentration, the conductivity change in the presence of NO was significantly lower. Likewise, the relative response of PS to interfering species (CO (up to 1000 ppm) and CH_4 (up to 5000 ppm)) and alcohol, such as methanol, at concentrations up to 800 ppm was negligible. They also used FTIR spectroscopy for detecting NO_2 through PSL which is studied in 2.1.1 section in details.

3. Conclusion

In this chapter, we presented a review work on the recent progress of PhC-based gas sensing research in the mid-infrared range. Various material structures including using porous silicon structure, photonic crystal waveguides, and hollow-core photonic crystal fibers, as well as both optical and electrical detection methods, have been thoroughly discussed. As mentioned, porous silicon structure enhanced sensing device achieved the highest sensitivity to detect NO_2 at 1 ppm concentration level through measuring the conductance changes. But this method is restricted to a limited range of gases, and is unable to detect nonpolar gases such as CO, CH_4, and alcohols. The other issue can be related to electrical components which are necessary for this method. These electrical components increase the risk of electrical discharge and augment the risk of explosion. Moreover, the electrical noises can strongly affect this kind of sensors. For the holey PCW, the sensor unit can deliver the measurement of Triethyl phosphate (TEP) with the concentration of 10 ppm. The small size (800 μm) of this PCW offers a great advantage which can potentially lead to the realization of SWaP sensors. The main drawback of this kind of sensors is that they are so sensitive to small fluctuation in the hole diameter. Thus, the fabrication process for this kind of sensors might be difficult and time-consuming. However, the high energy overlap with gases within the holey PCWs, and its high power in slowing light and its small size make this sensor one of the

best candidates for gas sensing applications. While, compared to the PCW, the PBF shows more electrical overlap with gases and lower propagation loss. Generally speaking, the development of PhC-based mid-infrared gas sensing research is still in its early stage and not ready for commercialization. However, considering the strong demands from IoT infrastructure for modern sensor units with combined SWaP-C features, it is anticipated that the progress in the PhC-based mid-infrared gas sensing area will develop much faster in the coming years, and some of the discussed technical approaches could eventually advance to a practical level and make a significant impact to our daily life.

Author details

Tahere Hemati and Binbin Weng*
School of Electrical and Computer Engineering, University of Oklahoma, Norman, OK, United States

*Address all correspondence to: binbinweng@ou.edu

IntechOpen

References

[1] Azad A, Akbar S, Mhaisalkar S, Birkefeld L, Goto K. Solid-state gas sensors: A review. Journal of the Electrochemical Society. 1992;**139**(12):3690-3704

[2] Eranna G, Joshi B, Runthala D, Gupta R. Oxide materials for development of integrated gas sensors a comprehensive review. Critical Reviews in Solid State and Materials Sciences. 2004;**29**(3-4):111-188

[3] Shimizu Y, Egashira M. Basic aspects and challenges of semiconductor gas sensors. MRS Bulletin. 1999;**24**(6):18-24

[4] Jaaniso R, Tan OK. Semiconductor Gas Sensors. Amsterdam: Elsevier; 2013

[5] Krebs P, Grisel A. A low power integrated catalytic gas sensor. Sensors and Actuators B: Chemical. 1993;**13**(1-3):155-158

[6] Spetz A, Winquist F, Sundgren H, Lundstrom I. Field effect gas sensors. In: Gas Sensors. University of Brescia, Italy: Springer; 1992. pp. 219-279

[7] Schmidt JC, Campbell DN, Clay SB. Electrochemical Gas Sensor. June 25 1985. US Patent 4,525,266

[8] Hodgkinson J, Tatam RP. Optical gas sensing: A review. Measurement Science and Technology. 2012;**24**(1):012004

[9] Sberveglieri G. Gas Sensors: Principles, Operation and Developments. University of Brescia, Italy: Springer Science & Business Media; 2012

[10] Gubbi J, Buyya R, Marusic S, Palaniswami M. Internet of things (IoT): A vision, architectural elements, and future directions. Future Generation Computer Systems. 2013;**29**(7):1645-1660

[11] Jones KH, Gross JN. Reducing size, weight, and power (swap) of perception systems in small autonomous aerial systems. In: 14th AIAA Aviation Technology, Integration, and Operations Conference. 2014. p. 2705

[12] Lambrecht A, Hartwig S, Schweizer S, Wehrspohn R. Miniature infrared gas sensors using photonic crystals. In: Photonic Crystal Materials and Devices VI. Vol. 6480. San Jose, California, United States: International Society for Optics and Photonics; 2007. p. 64800D

[13] Gao Y, Shiue RJ, Gan X, Li L, Peng C, Meric I, et al. High-speed electro-optic modulator integrated with graphene-boron nitride heterostructure and photonic crystal nanocavity. Nano Letters. 2015;**15**(3):2001-2005

[14] Ge X, Shi Y, He S. Ultra-compact channel drop filter based on photonic crystal nanobeam cavities utilizing a resonant tunneling effect. Optics Letters. 2014;**39**(24):6973-6976

[15] Fasihi K. High-contrast all-optical controllable switching and routing in nonlinear photonic crystals. Journal of Lightwave Technology. 2014;**32**(18):3126-3131

[16] Lin CY, Subbaraman H, Hosseini A, Wang AX, Zhu L, Chen RT. Silicon nanomembrane based photonic crystal waveguide array for wavelength-tunable true-time-delay lines. Applied Physics Letters. 2012;**101**(5):051101

[17] Yablonovitch E. Inhibited spontaneous emission in solid-state physics and electronics. Physical Review Letters. 1987;**58**(20):2059

[18] John S. Strong localization of photons in certain disordered dielectric superlattices. Physical Review Letters. 1987;**58**(23):2486

[19] Joannopoulos JD, Johnson SG, Winn JN, Meade RD. Photonic Crystals: Molding the Flow of Light. Princeton, New Jersey: Princeton University Press; 2011

[20] Notomi M. Strong light confinement with periodicity. Proceedings of the IEEE. 2011;**99**(10):1768-1779

[21] Yablonovitch E. Inhibited spontaneous emission in solid-state physics and electronics. Physics Review Letters. 1987;**58**:2059

[22] John S. Strong localization of photons in certain disordered dielectric superlattices. Physics Review Letters. 1987;**58**:2486

[23] Li H, Chang L, Wang J, Yang L, Song Y. A colorful oil-sensitive carbon inverse opal. Journal of Materials Chemistry. 2008;**18**(42):5098-5103

[24] Snow P, Squire E, Russell PSJ, Canham L. Vapor sensing using the optical properties of porous silicon Bragg mirrors. Journal of Applied Physics. 1999;**86**(4):1781-1784

[25] Lee K, Asher SA. Photonic crystal chemical sensors: Ph and ionic strength. Journal of the American Chemical Society. 2000;**122**(39):9534-9537

[26] Zhang YN, Zhao Y, Lv RQ. A review for optical sensors based on photonic crystal cavities. Sensors and Actuators A: Physical. 2015;**233**:374-389

[27] Xu H, Wu P, Zhu C, Elbaz A, Gu ZZ. Photonic crystal for gas sensing. Journal of Materials Chemistry C. 2013;**1**(38):6087-6098

[28] Nicoletti S. Mid-Infrared Photonics Devices Fabrication for Chemical Sensing and Spectroscopic Applications. Alpexpo in Grenoble, France: Semicon Europa; 2016

[29] Soref R. Mid-infrared photonics in silicon and germanium. Nature Photonics. 2010;**4**(8):495

[30] Seddon AB. A prospective for new mid-infrared medical endoscopy using chalcogenide glasses. International Journal of Applied Glass Science. 2011;**2**(3):177-191

[31] Reimer C, Nedeljkovic M, Stothard DJ, Esnault MO, Reardon C, O'Faolain L, et al. Mid-infrared photonic crystal waveguides in silicon. Optics Express. 2012;**20**(28):29361-29368

[32] Stuart B. Infrared Spectroscopy. Sydney, Australia: Wiley Online Library; 2005

[33] Korotcenkov G. Handbook of Gas Sensor Materials: Properties, Advantages and Shortcomings for Applications. Vol. 2. Gwangju, South Korea: New Trends and Technologies; 2014

[34] Hvozdara L, Gianordoli S, Strasser G, Schrenk W, Unterrainer K, Gornik E, et al. Spectroscopy in the gas phase with gaas/algaas quantum-cascade lasers. Applied Optics. 2000;**39**(36):6926-6930

[35] Pergande D, Geppert TM, Rhein Av, Schweizer SL, Wehrspohn RB, Moretton S, et al. Miniature infrared gas sensors using photonic crystals. Journal of Applied Physics. 2011;**109**(8):083117

[36] Jensen KH, Alam M, Scherer B, Lambrecht A, Mortensen NA. Slow-light enhanced light-matter interactions with applications to gas sensing. Optics Communications. 2008;**281**(21):5335-5339

[37] Conteduca D, Dell'Olio F, Ciminelli C, Armenise M. New miniaturized exhaled nitric oxide sensor based on a high q/v mid-infrared

1dphotonic crystal cavity. Applied Optics. 2015;**54**(9):2208-2217

[38] Chen Y, Lin H, Hu J, Li M. Heterogeneously integrated silicon pho-tonics for the mid-infrared and spectroscopic sensing. ACS Nano. 2014;**8**(7):6955-6961

[39] Milosevic MM, Nedeljkovic M, Ben Masaud TM, Jaberansary E, Chong HM, Emerson NG, et al. Silicon waveguides and devices for the mid-infrared. Applied Physics Letters. 2012;**101**(12):121105

[40] Boarino L, Baratto C, Geobaldo F, Amato G, Comini E, Rossi A, et al. No_2 monitoring at room temperature by a porous silicon gas sensor. Materials Science and Engineering B. 2000;**69**:210-214

[41] Kraeh C, Martinez-Hurtado J, Popescu A, Hedler H, Finley JJ. Slow light enhanced gas sensing in photonic crystals. Optical Materials. 2018;**76**:106-110

[42] Zou Y, Chakravarty S, Xu X, Lai W, Chen RT. Silicon chip based near-infrared and mid-infrared optical spectroscopy for volatile organic compound sensing. In: Lasers and Electro-Optics (CLEO), 2014 Conference on. San Jose, CA, USA: IEEE; 2014. pp. 1-2

[43] Lai WC, Zou Y, Chakravarty S, Zhu L, Chen RT. Comparative sensitivity analysis of integrated optical waveguides for near-infrared 14 volatile organic compounds with 1ppb detection. In: Silicon Photonics IX. Vol. 8990. San Francisco, California, United States: International Society for Optics and Photonics; 2014. p. 89900Z

[44] Ranacher C, Consani C, Tortschanoff A, Jannesari R, Bergmeister M, Grille T, et al. Mid-infrared absorption gas sensing using a silicon strip waveguide. Sensors and Actuators A: Physical. 2018;**277**:117-123

[45] Zou Y, Chakravarty S, Wray P, Chen RT. Mid-infrared holey and slotted photonic crystal waveguides in silicon-on-sapphire for chemical warfare simulant detection. Sensors and Actuators B: Chemical. 2015;**221**:1094-1103

[46] Rostamian A, Guo J, Chakravarty S, Chung C-J, Nguyen D, Chen RT. Parts-per-billion carbon monoxide sensing in silicon-on-sapphire mid-infrared photonic crystal waveguides. In: CLEO: Applications and Technology. San Francisco, California, United States: Optical Society of America; 2018. p. ATh1O–4

[47] Rajan G. Optical Fiber Sensors: Advanced Techniques and Applications. Vol. 36. Vancouver, British Columbia, Canada: CRC Press; 2015

[48] Knight JC, Broeng J, Birks TA, Russell PSJ. Photonic band gap guidance in optical fibers. Science. 1998;**282**:1476-1478

[49] Smith CM, Venkataraman N, Gallagher MT, Müller D, West JA, Borrelli NF, et al. Low-loss hollow-core silica/air photonic bandgap fibre. Nature. 2003;**424**:657-659

[50] Roberts PJ, Couny F, Sabert H, Mangan BJ, Williams DP, Farr L, et al. Ultimate low loss of hollow-core photonic crystal fibres. Optics Express. 2005;**13**:236-244

[51] Saini TS, Kumar A, Sinha RK. Broadband mid-infrared super-continuum spectra spanning 2-15 μm using as 2 se 3 chalcogenide glass triangular-core graded-index photonic crystal fiber. Journal of Light wave Technology. 2015;**33**(18):3914-3920

[52] Russell PSJ. Photonic-crystal fibers. Journal of Lightwave Technology. 2006;**24**:4729-4749

[53] Gayraud N, Stone JM, MacPherson WN, Shephard JD, Maier RRJ, Knight JC, et al. Mid infrared gas sensing using a hollowcore photonic bandgap fibre. In: Optical Fiber Sensors, OSA Technical Digest (CD). Cancun Mexico: Optical Society of America; 2006. paper ThA5

[54] Shephard JD, MacPherson WN, Maier RR, Jones JDC, Hand DP, Mohebbi M, et al. Single-mode mid-IR guidance in a hollowcore photonic crystal fiber. Optics Express. 2005;**13**:7139-7144

[55] Gayraud N, Kornaszewski LW, Stone JM, Knight JC, Reid DT, Hand DP, et al. Mid-infrared gas sensing using a photonic bandgap fiber. Applied Optics. 2008;**47**(9):1269-1277

[56] Bragg WH, Bragg BWL, et al. The reflection of x-rays by crystals. Proceedings of the Royal Society of London A. 1913;**88**(605):428-438

[57] Asher SA, Holtz J, Liu L, Wu Z. Self-assembly motif for creating submicron periodic materials. Polymerized crystalline colloidal arrays. Journal of the American Chemical Society. 1994;**116**(11):4997-4998

[58] Kobler J, Lotsch BV, Ozin GA, Bein T. Vapor-sensitive bragg mirrors and optical isotherms from mesoporous nanoparticle suspensions. ACS Nano. 2009;**3**(7):1669-1676

[59] Yang H, Jiang P. Macroporous photonic crystal-based vapor detectors created by doctor blade coating. Applied Physics Letters. 2011;**98**(1):011104

[60] Lu G, Farha OK, Kreno LE, Schoenecker PM, Walton KS, Van Duyne RP, et al. Fabrication of metal-organic framework-containing silica-colloidal crystals for vapor sensing. Advanced Materials. 2011;**23**(38):4449-4452

[61] Turduev M, Giden IH, Babayigit C, Hayran Z, Bor E, Boztug C, et al. Mid-infrared T-shaped photonic crystal waveg-uide for optical refractive index sensing. Sensors and Actuators B: Chemical. 2017;**245**:765-773